Calcification of abdominal aorta is an underappreciated cardiovascular disease risk factor.

Anurag Sethi[1,2], Leland Taylor[1,3], J Graham Ruby[2,4], Jagadish Venkataraman[2,4], Madeleine Cule[2,5], Eugene Melamud[2,5]

Abstract:

Background:

Calcification of the abdominal artery is an important contributor to cardiovascular disease in diabetic and chronic kidney disease (CKD) populations. However, prevalence of the pathology, risk factors, and long term disease outcomes in a general population have not been systematically analyzed.

Method:

We developed machine learning models to quantify levels of abdominal aortic calcification (AAC) in 29,957 whole body dual-energy X-ray absorptiometry (DEXA) scans from the UK Biobank cohort. Using regression techniques we associated severity of calcification across a wide range of physiological parameters, clinical biomarkers, and environmental risk factors (406 in total). We performed a common variant genetic association study spanning 9,572,557 single-nucleotide polymorphisms to identify genetic loci relevant to AAC. We evaluated the prognostic value of AAC across 151 disease classes using Cox proportional hazard models. We further examined an epidemiological model of calcification on cardiovascular morbidity with and without LDL interactions.

Findings:

We find evidence for AAC in >10.4% of the cohort despite low prevalence of diabetes (2.5%) and CKD (0.5%). Increased level of AAC is a strong prognostic indicator of cardiovascular outcomes for stenosis of precerebral arteries (HR~1.5), Myocardial Infarction (HR~1.5), & Ischemic Heart Disease (HR~1.33). We find that AAC is genetically

[1] These authors contributed equally
[2] Calico Life Sciences, LLC
[3] Current Address: Wellcome Sanger Institute
[4] These authors contributed equally
[5] Corresponding author

correlated with cardiovascular-related traits and that the genetic signals are enriched in vascular and adipose tissue. We report three loci associated with AAC, with the strongest association occuring at the *TWIST1*/*HDAC9* locus (beta=0.078, p-value=1.4e-11) in a region also associated with coronary artery disease. Surprisingly, we find that elevated but still within clinically normal levels of serum phosphate and glycated hemoglobin are linked to increased vascular calcification. Furthermore, we show AAC arises in the absence of hypercholesterolemia. By our estimate, AAC is an LDL-independent risk factor for cardiovascular outcomes, with risk similar to elevated LDL.

Data: This research has been conducted using the UK Biobank Resource.

Introduction:

Calcification of the vasculature is a commonly observed pathology in patients with end stage renal disease (ESRD) and diabetes (Giachelli 2004). At least two distinct forms of vascular calcification are known to exist - intimal layer calcification associated with atherosclerotic plaque and medial layer calcification internal to the tunica media layer of blood vessels. Intimal layer calcification is attributed to inflammatory hypercholesterolemia and calcification of plaque deposits, while medial layer calcification is attributed to growth of hydroxyapatite crystals within the blood vessel walls as a consequence of hyperphosphatemia and/or hypercalcemia (Lanzer et al. 2014; Amann 2008).

Although calcification can occur in all major arterial blood vessels, the prevalence of this pathology is site specific, and due to lack of routine monitoring, progression of calcification across various sites is hard to ascertain. In populations with high to moderate cardiovascular risk, the most commonly monitored sites are in the coronary artery calcification (CAC) via computed tomography measurement and in the carotid artery via ultrasound measurement. At both sites, calcification has been linked to degree of atherosclerosis and severity of calcification was found to be a prognostic indicator of poor cardiovascular outcomes. (Kelkar Anita A. et al. 2016; Prabhakaran et al. 2007; Budoff et al. 2007).

In this study, we present the largest epidemiological and genetic analysis of AAC to date. Using machine learning (ML) models, we developed an automated method to quantify level of AAC in 29,957 DEXA scans from the UK Biobank (UKBB) cohort. This cohort is approximately representative of the overall health status of middle age to eldery UK population (Keyes and Westreich 2019). To date more than 30,000 DEXA images have been collected and up to 100,000 will be collected in the next five years.

Leveraging the extensive measures of biomarkers and disease outcomes in UKBB, we estimate the contribution of hyperlipidemia, hyperphosphatemia, hypercalcemia, diabetes, and kidney health to the severity of AAC (Doherty et al. 2004). We utilize genotype data to identify and characterize genetic loci associated with AAC. Finally, using prospective electronic records, we report the association of AAC with risk of development of the most common diseases over an eight-year median follow up time.

Our analysis suggests that AAC arises as a consequence of transformation of arterial tissue into an osteogenic-like state, due to a combination of genetic drivers of vascular osteogenesis and age dependent physiological imbalances in the calcium-phosphate regulatory network. We find that calcification of abdominal aorta is a strong prognostic indicator of cardiovascular morbidity and show that this pathology can occur in the general population (not enriched for specific disease states).

Results:

Baseline Characteristics of Cohort:

The UKBB imaging study aims to generate detailed images on 100,000 of the 502,604 total UKBB participants by 2023 (Petersen et al. 2013). These images span a variety of modalities including DEXA scans of the whole body and targeted regions such as the upper torso. As of 1 March 2020, 48,670 participants have participated in the imaging cohort. In the latest (October 2019) release, DEXA scans were released for 31,494 participants. We were able to quantify AAC on 29,957 participants, herein referred to as the “calcification subcohort.”

We characterized the entire UKBB cohort and these 29,957 participants across a variety of measures ascertained at time of recruitment and, when available, at time of imaging (~8 years after initial recruitment; Table 1). Basic anthropometric and clinical measures revealed few differences between the calcification subcohort and the entire UKBB cohort.

We calculated the percentage of participants with comorbidities based on inpatient hospital records (ICD10 only; main or secondary diagnoses; Field 41270) at any time prior to the baseline visit, and also at any time prior to the imaging visit for the calcification subcohort. Compared to the entire UKBB cohort, the calcification subcohort exhibited slightly fewer comorbidities. Within the calcification subcohort, comorbidities increased in the ~8 years that spanned between recruitment and imaging recall. Overall,

the calcification subcohort was mostly free of inpatient diagnosis with only 2.8% of participants diagnosed with diabetes and 0.5% with CKD.

Finally, we analyzed biomarkers data from the date of initial recruitment into the UKBB cohort and found that most of the calcification subcohort had values within normal ranges, with frequencies of hyperphosphatemia (Phosphate>1.46 mmol/L) at 2.4%, hypercalcemia (Calcium>2.5 mmol/L) at 7.9% , hypercholesterolemia (LDL>190 mg/dL) at 6.15%, and hypervitaminosis D (25(OH)D3>140 ng/mL) at 0.06%.

Automatic Quantification of Abdominal Aortic Calcification:

Four annotators quantified AAC in 1,300 randomly chosen participants by assessing lateral DEXA scans of lumbar spine (**Figure S1 and Tables S1-S2**). We used a previously established scoring method (Kauppila et al. 1997), where each segment of abdominal aorta adjacent to the L1-L4 vertebra is given a score from 0 to 6. The individual scores for each segment are summed for a maximum score of 24. Intra-annotator variability did not have a large effect on the median annotation scores (Pearsons' correlation 0.93, **Figure S2**). We used 1,000 manually annotated images to train ML models and withheld 300 images to test the accuracy of the models (Methods).

For the ML models, we first considered a single-step regression model to directly predict AAC scores from the images; however, such an approach performed poorly due to substantial background noise within the DEXA images (**Figure S3**). We therefore developed a three step process to isolate and score the aortic region while reducing background noise (**Figures 1 and S4-S12**):

1. Identify the lower lumbar vertebrae (segmentation model).
2. Extract the abdominal aortic region based on the segmented lumbar vertebrae.
3. Use the abdominal aortic region to predict AAC scores (regression model).

We developed two independent pipelines to perform each of these steps (Methods). Each pipeline achieved similar accuracy on the test dataset (Pearson's correlation~0.6), but an ensemble score, generated by averaging the score of each pipeline, exhibited the best performance on the test dataset (Pearson's correlation~0.67; **Table 2 and Figure 2**). We therefore used the ensemble method to predict AAC scores in the whole dataset (29,957 images).

The distribution of calcification scores in the cohort was highly skewed towards low values (**Figure 2E**); the majority of participants (~88%) had no detectable or mild calcification (score< 3), with a long tail, defined as >1 standard deviation from the mean, representing ~12.3% of the population. We confirmed these estimates in the manually annotated subset of scans, where a comparable fraction (~10.4%) had moderate to high calcification (AAC score > 3). Both AAC severity and variability increased with age (**Figure 2F**). To our knowledge this is the first estimate of AAC prevalence from a large cohort not enriched for a specific disease. While it is known that prevalence of medial layer calcification in patients with diabetes and ESRD can be as high as 41% (Lanzer et al. 2014), we were surprised to observe such high prevalence in UKBB given that only 3.3% of the cohort has CKD and diabetes at baseline.

Risk factors for Abdominal Aortic Calcification:

We sought to identify potential risk factors for calcification with molecular biomarkers, physiological parameters, and complete blood cell counts (CBC) measures. We performed a univariate risk analysis with two different models: (i) adjusted for age and sex and (ii) adjusted for age, sex, BMI, socioeconomic factors, and smoking status (**Figures 3, S13-S14 and Table S4**).

Association with Biomarkers

After multiple hypothesis correction, we found that higher levels of glycated hemoglobin (HbA1c), phosphate, glucose, triglycerides, and gamma glutamyltransferase (GGT) in the serum are associated with increased AAC (**Figure 3 and Table S4)**. Four of the five associated biomarkers (HbA1c, glucose, triglycerides, and GGT) tend to be higher in diabetic patients, an observation that is consistent with diabetes being a risk factor for AAC (Stabley John N. and Towler Dwight A. 2017).

Calcification is known to occur in ESRD patients due to phosphate dysregulation (Craver et al. 2007). However, in our study we find that the majority of participants (~96.8%) with significant AAC are not hyperphosphatemic (serum phosphate > 1.46mM/liter, **Figure S15**). Furthermore, we observe that AAC is anticorrelated with creatinine levels (FWER p-value=5.7e-5) and is not associated with cystatin C. We estimated glomerular filtration rates (eGFR) from the cystatin C levels for all participants (FWER p-value = 1) (Methods). Across the first four quintiles of AAC, eGFR estimates were within normal kidney function ranges (eGFR ~90, **Figure S16**). Participants in the highest quintile of AAC were older and had slightly reduced kidney function (eGFR ~80). Given the low prevalence of CKD in this cohort (<0.5%), these results strongly suggest that calcification of abdominal arteries can occur in the absence of severe kidney disease.

We also observe that AAC is anticorrelated with high density lipoproteins (HDLs) (FWER p-value=1.29e-7), and not associated with low density lipoproteins (LDL) (FWER p-value = 1). Presence of AAC in the absence of hypercholesterolemia and lack of association with LDL is consistent with the hypothesis that AAC is likely to be a medial layer type of calcification (Szulc 2016). We further explore the independent nature of AAC and LDL using a variety of epidemiological models to predict myocardial infarction outcomes in the final section of this study.

Association with Complete Blood Cell Count:

Previous studies describe the frequent co-occurrence of calcification and inflammation (reviewed in (Demer and Tintut 2014)). We assessed the relationship between AAC and CBC measures (**Figure 3 & Table S5)** and found AAC was positively correlated with markers of inflammation. Specifically, AAC was associated with increased cell counts of white blood cells, neutrophils, monocytes, platelets, and reticulocytes. In addition, AAC was correlated with increased mean corpuscular volume and hemoglobin concentration of red blood cells.

Association with Physiological Markers

,We also identified several associations between AAC and physiological parameters (cutoff FWER p-value<1.2e-4; **Figure 3 & Table S6)**. AAC was most strongly associated with increased intima medial thickness (IMT) of the carotid artery, which occurs due to build up of plaque and/or calcification within this artery, suggesting that calcification within the carotid artery is correlated with AAC. As expected, increased AAC was correlated with increased systolic blood pressure, increased ventricular rate (Rubin et al. 2012), decreased bone mineral density (Shavit et al. 2015), decreased forced vital capacity, and decreased forced expiratory volume (McAllister et al. 2011). Overall, after taking into account age related decline, presence of aortic calcification was associated with reduced physiological function across a number of organ systems.

We carried out a replication study in the MrOS cohort to confirm biochemical and physiological associations with AAC (Szulc et al. 2014). All major UKBB findings showed comparable associations in MrOS, including: increased level of AAC with phosphate, HbA1C, glucose, triglycerides, systolic blood pressure, as well as anticorrelation with HDL (Figure S13).

Genetic architecture of AAC

To identify genetic contributors to AAC, we performed a common variant genome wide association study (GWAS), testing 9,572,557 single-nucleotide polymorphisms (SNPs) across 25,411 participants (Methods). We identified three associated loci ($P<5x10^{-8}$; Figure 4A) and estimated the SNP based heritability (h_g^2) to be 15.4% (s.e. 0.02%). To identify tissues and cell types relevant to AAC we partitioned the heritability of AAC genetic signals across the genome using tissue/cell type annotations derived from chromatin marks and marker genes (Methods). After multiple hypothesis correction, we found enrichment of heritability in blood vessels, vascular endothelial cells, subcutaneous fat, visceral fat, and breast tissue (FDR<5%; Figure 4B, Figure S17).

We calculated the genetic correlation between AAC and 836 other traits (Methods). AAC was genetically correlated (FDR<0.05) with diabetes as well as 15 cardiovascular-related diseases, traits, and medications, suggesting a common set of genetic risk factors among these phenotypes (Figure 4C; Supplementary Figure S20; Supplementary Table Tab 8). Notably, we did not find evidence of genetic correlation for other phenotypes identified as correlated with AAC in this study including inflammation markers, lung function, or lipid levels. Such results may indicate independent genetic risk factors for these phenotypes; however, lack of power may also explain these results.

Identification of AAC-associated loci.

To better understand the biological mechanisms at each of the three identified loci, we performed in-depth analyses at each locus (Methods). First, to identify potential causal variants, we performed conditional and credible set analysis. Second, to identify candidate effector genes, we performed colocalization analysis using associations with gene expression (i.e., expression quantitative trait loci; eQTLs) from GTEx v7. Finally, to identify other diseases and traits that likely share the same underlying causal variant, we performed genetic colocalization analysis using UKBB phenotypes that have an association (p-value<5e-8) within 500kb of the lead SNP.

At the rs1065853 locus (p-value=2.9e-9), we identified no secondary associations and 19 SNPs within the 95% credible set. We found no evidence for colocalization with the expression of any gene in any tissue; however, we did find strong evidence of colocalization with traits related to heart disease, red blood cell measurements, and dietary traits (Supplementary Tables 4-7). Given that the lead SNP, rs1065853, is in linkage disequilibrium ($r^2>0.99$) with the APOE e2 allele, rs7412, these results are

consistent with the well-established role of APOE and lipid metabolism (Eichner et al. 2002); however, the link with AAC is less clear and warrants further investigation in future studies.

At the rs201299446 locus on chromosome two (p-value=2.2e-8), we identified no secondary associations and 35 SNPs within the 95% credible set. We found no evidence for colocalization with gene expression, other diseases, or other quantitative traits.

At the rs2107595 locus (p-value=1.4E-11), we identified seven SNPs within the 95% credible set, all of which lie in a non-coding region near *HDAC9* and *TWIST1*. The SNP with the largest posterior probability of association (0.77), rs2107595, lies in a promoter flanking region (ENSR00000818178) active in cell types related to smooth muscle, bone, and epithelial tissue and strongly disrupts a predicted transcription factor (TF) binding site for the E2F family of TFs and ZNF75A (http://ensembl.org).

This AAC signal colocalizes with *TWIST1* expression in aortic artery (Figure 5, Figure S18), but not with *HDAC9* expression in any tissue. We tested if either *TWIST1* or *HDAC9* expression was correlated with calcification diagnosis from GTEx histological images of vascular tissue. We found *TWIST1* expression was associated with tibial artery calcification (beta=0.265, SE=0.0649, $\text{p-value}_{\text{Bonferroni}}$=0.0002616), but not *HDAC9* in any tissue considered (minimum $\text{p-value}_{\text{Bonferroni}}$=0.2488).

We explored mouse aorta single cell expression data (Methods) and found *Twist1* was highly expressed in fibroblasts, vascular smooth muscle cells, and endovascular progenitor endothelial cells that also express mesenchymal marker genes (Figure S19). Finally, we also found strong evidence of colocalization between this AAC signal and several cardiovascular phenotypes: coronary artery disease (CAD), ischemic heart disease, occlusion and stenosis of precerebral arteries, and systolic blood pressure (SBP; Figure 4c; Supplementary Table Tab 8).

While we cannot draw causal conclusions of the relationship between *TWIST1*, AAC, SBP, and CAD, one hypothesis consistent with our observations is that rs2107595 increases *TWIST1* expression in vascular cells, which increases AAC, leading to increased SBP and CAD risk. Such a hypothesis is consistent with the observed increase of TWIST1 in adult human calcified aortic valves (Wirrig, Hinton, and Yutzey 2011; Chakraborty et al. 2010), the possible role of *Twist1* in promoting endothelial–mesenchymal transitions that drive vascular calcification (Yao et al. 2015), and theories that vascular calcification can be caused by progenitor cells (reviewed in (Leszczynska and Murphy 2018; Xie et al. 2019; Hortells, Sur, and St Hilaire 2018)).

Aortic Calcification is a prognostic measure for cardiovascular, cerebrovascular, and lung related chronic diseases:

The EHR of most UKBB participants is available and these records extend to approximately 8.27 years post baseline (median followup time). We estimated the prognostic value of AAC using a Cox proportional hazard (CoxPH) model (Cox 1972) on 151 disease classes (Methods). We considered two models: (i) adjusted for age and sex (Model1) and (ii) adjusted for age, sex, BMI, socieconomic status, race, and smoking (Model 2).

After multiple hypothesis correction ($p\text{-value}_{Bonferroni}<0.05$), we find that AAC levels are a strong prognostic risk factor for cardiovascular morbidity across a number of disease classes including occlusion of precerebral arteries (HR~1.5), acute myocardial infarction (HR~1.5), chronic ischemic heart disease (HR~1.33), hypertension (HR~1.25), obstructive chronic bronchitis (HR~1.36), and gout (HR~1.25); **Figures 6 and S21**). These observations support the hypothesis that calcification of vasculature is a commonly shared disease pathophysiology that manifests in long term negative outcomes across the entire cardiovascular system.

To further investigate a hypothesis that AAC is a risk factor for myocardial infarction (MI) events independent of hypercholesterolemia, we used multivariate CoxPH models to compare additive risk and interactions between AAC and LDL. Because ~15% of the cohort have been prescribed statins, this model may underestimate the contribution of LDL, because the baseline measure will not account for lifetime exposure of LDL (HR_{LDL}~1.24, HR_{AAC}~1.4; Figure 7A). Therefore, to obtain an unbiased estimate for LDL and AAC MI risk, we estimated LDL risk after adjusting for statin usage using four different models (Methods; Figures S22-S24).

In the first model, we estimated LDL risk for statin nonusers. Since statin usage is recommended only for participants with hypercholesterolemia and higher pre-existing cardiovascular risk, we expect the estimates for LDL risk in this model is confounded by lack of hyperlipidemia diagnosis and is biased toward healthier populations. In models 2 and 3, we adjusted the LDL levels for statin users based on a previous report (Nissen et al. 2005) that estimates the use of statin reduces LDL levels by ~1.25 mmol/L (Model 2) or 35% (Model 3; **Figures 7,S22**). Finally, in model 4, we imputed the untreated LDL levels for statin users based on blood pressure, pulse, age, sex, and non-lipid molecular biomarkers (**Figure S24**).

In all four models, MI risk associated with severity of AAC (HR~1.4 per standard deviation) was comparable to LDL risk (HR~1.4 per standard deviation). We did not find evidence for an interaction between LDL and AAC (p-value>0.05) in any model, suggesting that AAC is a hypercholesterolemia-independent risk factor for MI. These results are also consistent with our genetic analysis which did not find genetic correlation between AAC and lipid biomarkers (Figure 4C; Supplementary Table Tab 8).

Discussion:

Vascular calcification is associated with cardiovascular morbidity and can arise as a complication of diabetes and chronic kidney disease (Giachelli 2004). It has been poorly studied in healthy individuals due to lack of routine monitoring and lack of tools to quantitate AAC. Here, we present one of the largest studies of AAC, spanning 29,957 participants from a biobank approximately representative of the general UK population. To enable this study, we developed a method to automatically quantify AAC from DEXA scans. Our method is publically available (https://github.com/calico/AAC_scoring) and accurately predicts severity of calcification as judged by comparison to manual quantifications.

In our study, we observed a high prevalence of AAC (>10% of participants), even though <3.3% of the cohort is diagnosed with CKD and diabetes. We found that severity of AAC is strongly associated with elevated serum phosphate and HbA1c, even though the levels of these biomarkers would be considered within clinically normal ranges. We found that aortic calcification was not associated with LDL, serum calcium, and vitamin D levels. These observations suggest that even in adults without diabetes and kidney disease, moderate elevation of serum phosphate and glucose levels are associated with higher risk of calcification and as a consequence cardiovascular outcomes. These results are consistent with similar observations made in the Framingham Offspring Study (Dhingra et al. 2007) that the risk for cardiovascular disease increases with phosphate levels even in the absence of hyperphosphatemia.

The physiological rationale for ossification of abdominal aorta in a largely healthy population is not clear. Calcium/phosphate balance is tightly regulated by complex interactions between the parathyroid gland, kidney, bone, and gut. Normal response to excess calcium and phosphate is to restore balance by increased renal clearance and absorption of excess ions into bones. However, if a normal physiological response cannot be achieved, it has been suggested that smooth muscle cells transform into osteoblast-like state and hydroxyapatite is progressively deposited across various parts

of cardiovascular system including heart valves, coronary arteries, aorta, abdominal aorta, tibial arteries, and kidneys (Sage, Tintut, and Demer 2010; Burton, Matsubara, and Ikeda 2010).

In support of this “phenotypic-switch” hypothesis, our analyses suggest that vascular cells play an important role in the development of AAC. First, we found enrichment of AAC heritability in regions near marker genes for blood vessels, vascular endothelial cells, and adipose tissue. Second, we discovered an AAC-associated locus (rs2107595; also associated with CAD and SBP), that our analysis suggests is mediated by an increase of *TWIST1* expression resulting in osteogenic phenotype within smooth muscle and/or vascular endothelial cells.

In addition to the exploration of the rs2107595 presented in this study, two recent studies investigated this locus in more depth. Nurnberg et al. (Nurnberg et al. 2020) found that disrupting the rs2107595 locus in coronary artery smooth muscle alters *TWIST1* expression and that *TWIST1* expression affects proliferation and calcification phenotypes in vascular smooth muscle cells.. Malhotra et al (Malhotra et al. 2019) also identified rs2107595 as a variant associated with atherosclerotic AAC and investigated the potential role for *HDAC9* in calcification of vascular smooth muscle cells. While we cannot exclude a role for *HDAC9* in this phenotype, our analysis supports at least some involvement of *TWIST1* at this locus.

Finally, we evaluated the role of calcification as a prognostic marker of disease outcomes. We found that the severity of AAC is strongly predictive of future MI, CHD, chronic obstructive bronchitis, gout, peripheral, and brain disorders. We further considered four epidemiological models to evaluate the independence of AAC and hypercholesterolemia. In all models, AAC was a separate additive contributor to MI outcomes, independent of LDL risk. We did not observe significant interaction in any of the models with LDL levels—supporting a hypothesis that AAC is not plaque driven but rather arises through conversion of smooth muscle cells to osteoblast-like cells and tunica media layer calcification.

Collectively, our results highlight the potential of a simple, non-invasive spine X-ray as a tool to assess the risk for a broad range of cardiovascular events, and warrants further investigation of routine AAC measurement as a prognostic indicator of cardiovascular disease. The strong link between AAC and cardiovascular outcomes, that is independent of hypercholesterolemia and statin usage, suggest that development of anti-calcification therapeutics could be complementary to lipid lowering strategies in reducing cardiovascular disease burden in a general population.

Acknowledgements

The authors would like to thank Nick van Bruggen, Garrett Fitzgerald, Aarif Khakoo, David Kelley, Magdalena Lopez, Tian-Quan Cai, and Dan Eaton for discussions and inputs regarding the manuscript. This research has been conducted using the UK Biobank Resource. This work was supported by Calico Life Sciences LLC.

Abbreviations:

HbA1c - glycated hemoglobin
GGT - gamma glutamyl transferase
ApoA - apolipoprotein
HDL - high density lipoprotein
LDL - low density lipoprotein
WBC - White blood cell
MCV - mean corpuscular volume
MCHC - mean corpuscular haemoglobin concentration
RBC - red blood cell, Imm.
Reticulocyte - immature reticulocyte
IMT - intima media thickness
SBP - systolic blood pressure
PEF - peak expiratory flow
FVC - forced vital capacity
QUI - quantitative ultrasound index, US- ultrasound
BMD - bone mineral density
FEV1 - forced expiratory volume in 1 second.

References

1. Amann, Kerstin. 2008. “Media Calcification and Intima Calcification Are Distinct Entities in Chronic Kidney Disease.” *Clinical Journal of the American Society of Nephrology: CJASN* 3 (6): 1599–1605.
2. Budoff, Matthew J., Leslee J. Shaw, Sandy T. Liu, Steven R. Weinstein, Tristen P. Mosler, Philip H. Tseng, Ferdinand R. Flores, Tracy Q. Callister, Paolo Raggi, and Daniel S. Berman. 2007. “Long-Term Prognosis Associated with Coronary Calcification: Observations from a Registry of 25,253 Patients.” *Journal of the American College of Cardiology* 49 (18): 1860–70.
3. Burton, D. G. A., H. Matsubara, and K. Ikeda. 2010. “Pathophysiology of Vascular Calcification: Pivotal Role of Cellular Senescence in Vascular Smooth Muscle Cells.” *Experimental Gerontology* 45 (11): 819–24.
4. Chakraborty, Santanu, Elaine E. Wirrig, Robert B. Hinton, Walter H. Merrill, Douglas B. Spicer, and Katherine E. Yutzey. 2010. “Twist1 Promotes Heart Valve Cell Proliferation and Extracellular Matrix Gene Expression during Development in Vivo and Is Expressed in Human Diseased Aortic Valves.” *Developmental Biology*. https://doi.org/10.1016/j.ydbio.2010.08.021.
5. Cox, D. R. 1972. “Regression Models and Life-Tables.” *Journal of the Royal Statistical Society. Series B, Statistical Methodology* 34 (2): 187–220.
6. Craver, Lourdes, Maria Paz Marco, Isabel Martínez, Montserrat Rue, Merce Borràs, Maria Luisa Martín, Felipe Sarró, José Manuel Valdivielso, and Elvira Fernández. 2007. “Mineral Metabolism Parameters throughout Chronic Kidney Disease Stages 1-5--Achievement of K/DOQI Target Ranges.” *Nephrology, Dialysis, Transplantation: Official Publication of the European Dialysis and Transplant Association - European Renal Association* 22 (4): 1171–76.
7. Dhingra, Ravi, Lisa M. Sullivan, Caroline S. Fox, Thomas J. Wang, Ralph B. D’Agostino Sr, J. Michael Gaziano, and Ramachandran S. Vasan. 2007. “Relations of Serum Phosphorus and Calcium Levels to the Incidence of Cardiovascular Disease in the Community.” *Archives of Internal Medicine* 167 (9): 879–85.
8. Doherty, Terence M., Lorraine A. Fitzpatrick, Daisuke Inoue, Jian-Hua Qiao, Michael C. Fishbein, Robert C. Detrano, Prediman K. Shah, and Tripathi B. Rajavashisth. 2004. “Molecular, Endocrine, and Genetic Mechanisms of Arterial Calcification.” *Endocrine Reviews* 25 (4): 629–72.
9. Eichner, June E., S. Terence Dunn, Ghazala Perveen, David M. Thompson, Kenneth E. Stewart, and Berrit C. Stroehla. 2002. “Apolipoprotein E Polymorphism and Cardiovascular Disease: A HuGE Review.” *American Journal of Epidemiology* 155 (6): 487–95.
10. Giachelli, Cecilia M. 2004. “Vascular Calcification Mechanisms.” *Journal of the American Society of Nephrology: JASN* 15 (12): 2959–64.
11. Hortells, Luis, Swastika Sur, and Cynthia St Hilaire. 2018. “Cell Phenotype Transitions in Cardiovascular Calcification.” *Frontiers in Cardiovascular Medicine* 5 (March): 27.
12. Kauppila, L. I., J. F. Polak, L. A. Cupples, M. T. Hannan, D. P. Kiel, and P. W. Wilson. 1997. “New Indices to Classify Location, Severity and Progression of Calcific Lesions in the Abdominal Aorta: A 25-Year Follow-up Study.” *Atherosclerosis* 132 (2): 245–50.

13. Kelkar Anita A., Schultz William M., Khosa Faisal, Schulman-Marcus Joshua, O'Hartaigh Briain W.J., Gransar Heidi, Blaha Michael J., et al. 2016. "Long-Term Prognosis After Coronary Artery Calcium Scoring Among Low-Intermediate Risk Women and Men." *Circulation. Cardiovascular Imaging* 9 (4): e003742.
14. Keyes, Katherine M., and Daniel Westreich. 2019. "UK Biobank, Big Data, and the Consequences of Non-Representativeness." *The Lancet* 393 (10178): 1297.
15. Lanzer, Peter, Manfred Boehm, Victor Sorribas, Marc Thiriet, Jan Janzen, Thomas Zeller, Cynthia St Hilaire, and Catherine Shanahan. 2014. "Medial Vascular Calcification Revisited: Review and Perspectives." *European Heart Journal* 35 (23): 1515–25.
16. Leszczynska, Aleksandra, and J. Mary Murphy. 2018. "Vascular Calcification: Is It Rather a Stem/Progenitor Cells Driven Phenomenon?" *Frontiers in Bioengineering and Biotechnology* 6 (February): 10.
17. Malhotra, Rajeev, Andreas C. Mauer, Christian L. Lino Cardenas, Xiuqing Guo, Jie Yao, Xiaoling Zhang, Florian Wunderer, et al. 2019. "HDAC9 Is Implicated in Atherosclerotic Aortic Calcification and Affects Vascular Smooth Muscle Cell Phenotype." *Nature Genetics* 51 (11): 1580–87.
18. McAllister, David A., William MacNee, Daniel Duprez, Eric A. Hoffman, Jens Vogel-Claussen, Michael H. Criqui, Matthew Budoff, Rui Jiang, David A. Bluemke, and R. Graham Barr. 2011. "Pulmonary Function Is Associated with Distal Aortic Calcium, Not Proximal Aortic Distensibility. MESA Lung Study." *COPD* 8 (2): 71–78.
19. Nissen, Steven E., E. Murat Tuzcu, Paul Schoenhagen, Tim Crowe, William J. Sasiela, John Tsai, John Orazem, et al. 2005. "Statin Therapy, LDL Cholesterol, C-Reactive Protein, and Coronary Artery Disease." *The New England Journal of Medicine* 352 (1): 29–38.
20. Nurnberg, Sylvia T., Marie A. Guerraty, Robert C. Wirka, H. Shanker Rao, Milos Pjanic, Scott Norton, Felipe Serrano, et al. 2020. "Genomic Profiling of Human Vascular Cells Identifies TWIST1 as a Causal Gene for Common Vascular Diseases." *PLoS Genetics* 16 (1): e1008538.
21. Petersen, Steffen E., Paul M. Matthews, Fabian Bamberg, David A. Bluemke, Jane M. Francis, Matthias G. Friedrich, Paul Leeson, et al. 2013. "Imaging in Population Science: Cardiovascular Magnetic Resonance in 100,000 Participants of UK Biobank - Rationale, Challenges and Approaches." *Journal of Cardiovascular Magnetic Resonance: Official Journal of the Society for Cardiovascular Magnetic Resonance* 15 (May): 46.
22. Prabhakaran, Shyam, Rajinder Singh, Xianhuang Zhou, Romel Ramas, Ralph L. Sacco, and Tatjana Rundek. 2007. "Presence of Calcified Carotid Plaque Predicts Vascular Events: The Northern Manhattan Study." *Atherosclerosis* 195 (1): e197–201.
23. Rubin, Jonathan, Michael J. Blaha, Matthew J. Budoff, Juan J. Rivera, Leslee J. Shaw, Ron Blankstein, Mouaz-Al Mallah, et al. 2012. "The Relationship between Resting Heart Rate and Incidence and Progression of Coronary Artery Calcification: The Multi-Ethnic Study of Atherosclerosis (MESA)." *Atherosclerosis* 220 (1): 194–200.
24. Sage, Andrew P., Yin Tintut, and Linda L. Demer. 2010. "Regulatory Mechanisms in Vascular Calcification." *Nature Reviews. Cardiology* 7 (9): 528–36.
25. Shavit, Linda, Daniela Girfoglio, Vivek Vijay, David Goldsmith, Pietro Manuel Ferraro, Shabbir H. Moochhala, and Robert Unwin. 2015. "Vascular Calcification and Bone Mineral Density in Recurrent Kidney Stone Formers." *Clinical Journal of the American Society of Nephrology: CJASN* 10 (2): 278–85.
26. Stabley John N., and Towler Dwight A. 2017. "Arterial Calcification in Diabetes Mellitus." *Arteriosclerosis, Thrombosis, and Vascular Biology* 37 (2): 205–17.
27. Szulc, Pawel. 2016. "Abdominal Aortic Calcification: A Reappraisal of Epidemiological and

Pathophysiological Data." *Bone* 84 (March): 25–37.
28. Szulc, Pawel, Terri Blackwell, John T. Schousboe, Douglas C. Bauer, Peggy Cawthon, Nancy E. Lane, Steven R. Cummings, Eric S. Orwoll, Dennis M. Black, and Kristine E. Ensrud. 2014. "High Hip Fracture Risk in Men with Severe Aortic Calcification: MrOS Study." *Journal of Bone and Mineral Research: The Official Journal of the American Society for Bone and Mineral Research* 29 (4): 968–75.
29. Wirrig, Elaine E., Robert B. Hinton, and Katherine E. Yutzey. 2011. "Differential Expression of Cartilage and Bone-Related Proteins in Pediatric and Adult Diseased Aortic Valves." *Journal of Molecular and Cellular Cardiology* 50 (3): 561–69.
30. Xie, Changming, Liu Ouyang, Jie Chen, Huanji Zhang, Pei Luo, Jingfeng Wang, and Hui Huang. 2019. "The Emerging Role of Mesenchymal Stem Cells in Vascular Calcification." *Stem Cells International* 2019 (April): 2875189.
31. Yao, Jiayi, Pierre J. Guihard, Ana M. Blazquez-Medela, Yina Guo, Jeremiah H. Moon, Medet Jumabay, Kristina I. Boström, and Yucheng Yao. 2015. "Serine Protease Activation Essential for Endothelial-Mesenchymal Transition in Vascular Calcification." *Circulation Research* 117 (9): 758–69.

Tables

	UKBB Cohort (baseline)	Calcification subcohort (baseline)	Calcification subcohort (imaging baseline)
n	502,604	29,957	29,957
Age (years)	56.3 (8.1)	54.9 (7.5)	63.3 (7.5)
% Females	54.40%	51.10%	51.10%
BMI	27.43 (4.80)	26.63 (4.23)	26.52 (4.36)
SBP	139 (20)	137 (19)	138 (18)
Pulse	68 (11.7)	68.0 (11.0)	69.2 (12.1)
Smoker (current)	10.50%	6.50%	3.68%
Smoker (previous)	34.50%	32.50%	33.67%
Comorbidities			
% Hypertension	7.88%	4.13%	12.66%
% T1D	0.42%	0.15%	0.28%
% T2D	1.83%	0.71%	2.52%
% MI	2.12%	1.12%	3.62%
% Stroke	0.14%	0.07%	0.11%
% CAD	0.99%	0.57%	1.30%
% CKD	0.13%	0.02%	0.50%
Biomarkers			
Glucose (mmol/L)	5.12 (1.24)	5.00 (0.98)	
HbA1c (mmol/mol)	35.2 (6.78)	35.0 (5.07)	
Trig (mmol/L)	1.75 (1.45)	1.67 (0.98)	
LDL (mmol/L)	3.56 (0.87)	3.58 (0.83)	
HDL (mmol/L)	1.45 (0.38)	1.47 (0.37)	
Cholesterol (mmol/L)	5.69 (1.14)	5.72 (1.09)	
Serum Phosphate (mmol/L)	1.16 (0.16)	1.15 (0.16)	
Serum Calcium (mmol/L)	2.38 (0.09)	2.37 (0.09)	
Serum Creatinine (umol/L)	72.31 (18.55)	72.63(14.16)	
Cystatin C (mg/L)	0.91 (0.18)	0.87 (0.13)	

Table 1: Baseline characteristics of the UK Biobank (UKBB) cohort and the calcification subcohort. The following second level ICD10 codes were used to identify the number of participants with different comorbidities: E10 - Type 1 Diabetes (T1D), E11 - Type 2 Diabetes (T2D), I25 - Myocardial Infarction (MI), I64 - Stroke, I21 - Coronary Artery Disease (CAD), and N18 - Chronic Kidney Disease (CKD). BMI - body mass index, SBP - systolic

blood pressure, HbA1c - glycated haemoglobin, Trig - triglycerides, LDL - low density lipoprotein, HDL - high density lipoprotein. The calcification cohort revisited the centers for imaging ~8 years after the baseline visit for all UKBB cohort participants.

	Pearson correlation with median score	**Spearman correlation with median score**
Annotator 1	0.94	0.83
Annotator 2	0.93	0.88
Annotator 3	0.85	0.84
Annotator 4	0.73	0.57
Machine Learning Models		
Model 1	0.62	0.41
Model 2	0.59	0.47
Ensemble Model	0.67	0.49

Table 2: Accuracy of machine learning pipelines. The accuracy of the machine learning pipelines and the ensemble model were calculated using Pearsons' and Spearman's correlation coefficient over the test dataset. Correlation of each individual annotator with the median for the test dataset is also shown for comparison.

Figure Captions

Figure 1 - Schematic of the machine learning pipeline to quantify AAC. Overview of the two independent machine learning pipelines used to quantify AAC. (A) Representative DEXA scan (manual annotation score = 15). (B) Pipeline 1: segmentation of the lower spine using U-Net architecture (blue). (C) Pipeline 2: box segmentation of individual lumbar vertebrae (blue). Extracted aortic regions are highlighted in orange in (B) and (C). (D) AAC scores are quantified using a neural network (NN) based regression against human-derived aortic calcification scores. An ensemble AAC score, combining predictions from both pipelines, performed the best in an unseen test dataset.

Figure 2- Comparison of machine learning based AAC scores to manually annotated AAC scores. (A) Correlation of manually annotated calcification scores with ensemble machine learning (ML) scores on the 300 test images. (B-D) Comparison of ML and manual scores for participants with low, medium and high levels of calcification within the test dataset. (E) Distribution of predicted AAC scores across 29,957 participants. (F) Relationship between predicted AAC scores and age of the participants. Red line in (A) and (E) indicates calcification score at 1 standard deviation (score=2.93).

Figure 3: Association of AAC with (A) molecular biomarkers, (B) CBC measures, and (C) physiological parameters. The blue dot represents the mean effect size, error bars represent 95% confidence interval. With the exception of LDL and cystatin C, only covariates that passed multiple hypothesis testing in model 1 are shown (Bonferroni corrected p-value<1.2e-4). We include LDL and cystatin C as they are discussed in the text.

Figure 4: Genetic analysis of AAC. (A) Manhattan plot. Association of each SNP -log(p-values) ordered by chromosome. Genome wide significance cut-off (p-value $5x10^{-8}$) shown as a red line. (B) AAC heritability enrichment and 95% confidence interval (y-axis) partitioned across tissue/cell type annotations (x-axis). Marked in black are tissues with heritability enrichment passing FDR<5%. In order from left to right: subcutaneous fat, subcutaneous adipose tissue (Adipose panel), visceral omentum (Adipose panel), subcutaneous fat in adipose tissue (Adipose panel); endothelial cells (Cardio panel), blood vessels in vascular tissue (Cardio panel); and breast tissue (Other panel). (C) Genetic correlation identified using LD Score Regression. Marked in black are correlations passing FDR<5%. We find positive correlation with presence of cardiometabolic traits, glycemic traits (diagnosis of Type 2 Diabetes), and medications.

Abbreviations: cardiovascular (Cardio), central nervous system (CNS), and musculoskeletal-connective (Musc). Coefficient estimates are shown in Figure S18.

Figure 5: Colocalization analysis at the *TWIST1/HDAC9* locus. (A) Association (y-axis) of genetic variants (x-axis) with AAC (red), the colocalizing UKBB diseases/traits (blue). Red dashed line denotes rs2107595. (B) Replication studies of the UKBB colocalizing diseases/traits. The two replication studies do not use UKBB participants. (C) Genetic association with the expression of nearby genes in aorta. Abbreviations: abdominal aortic calcification (AAC), coronary artery disease (CAD), occlusion and stenosis of precerebral arteries (O&S), systolic blood pressure (SBP), and diastolic blood pressure (DBP).

Figure 6: CoxPH association of AAC with prognosis of diseases. Hazard ratio for the subset of statistically significant disease associations after multiple hypothesis testing ($p\text{-value}_{Bonferroni}<0.05$). The blue dots represent mean hazard ratio, the error bars represent 95% confidence intervals.

Figure 7 - CoxPH association of AAC and LDL for acute MI events. We compared the hazard ratios for AAC, LDL, and triglycerides using a multivariate CoxPH model with age and sex covariates. (A) Whole cohort - no statin adjustment. (B) Subset of only non-statin users. (C) Whole cohort after adjusting for statin using method 1 - assumes that LDL levels are reduced by 1.25 mmol/L in statin users. (D) Whole cohort method 2 - assumes that LDL levels are reduced by 35% in statin users. (E) Whole cohort imputation of LDL levels based on remaining biomarkers and physiological measurements (Methods). The blue dots represent mean hazard ratio, while error bars represent 95% confidence interval. Interaction term between LDL and calcification is starred.

Figure 1

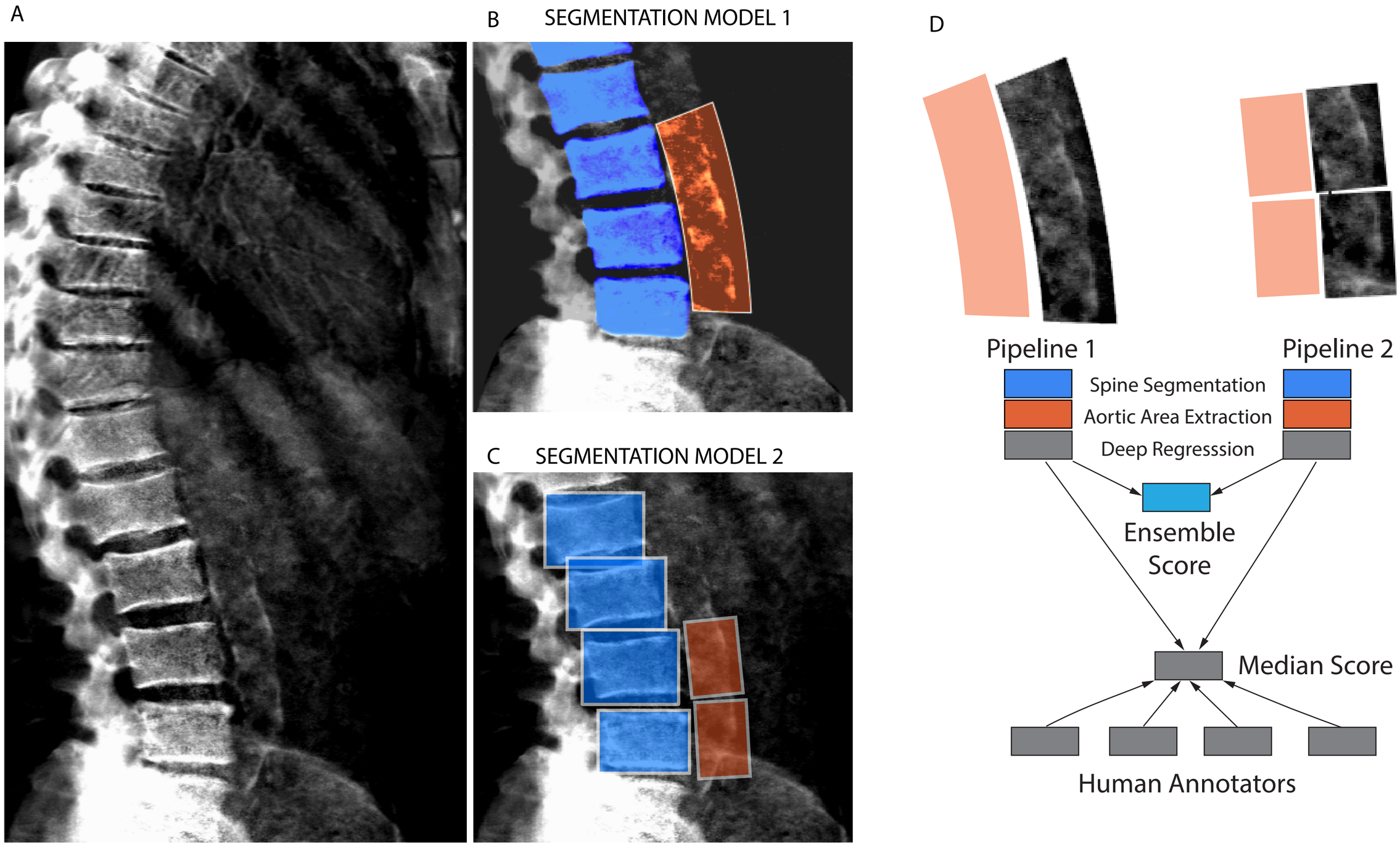
A
B
SEGMENTATION MODEL 1
C
SEGMENTATION MODEL 2
D
Pipeline 1
Pipeline 2
Spine Segmentation
Aortic Area Extraction
Deep Regresssion
Ensemble Score
Median Score
Human Annotators

Figure 2

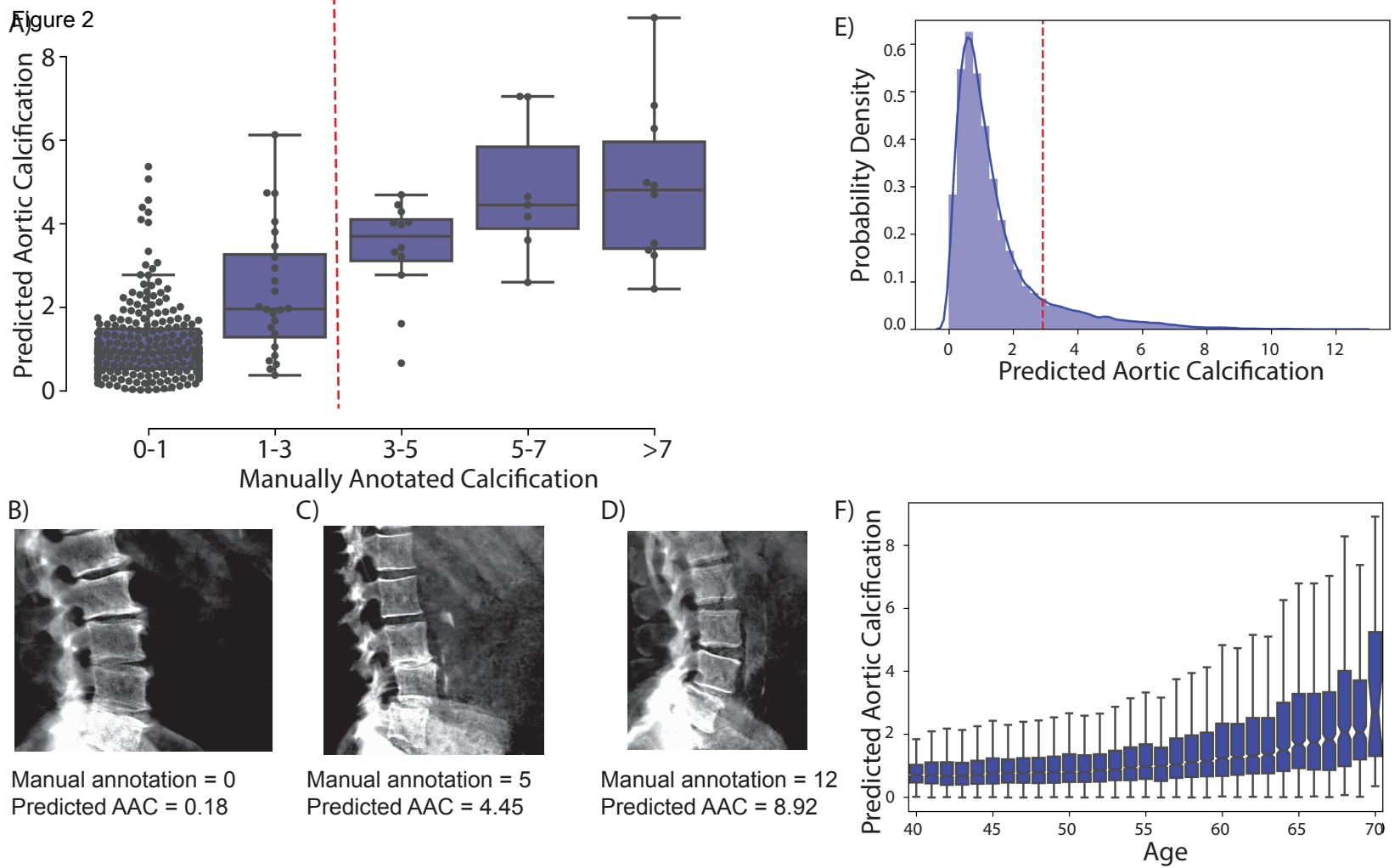
A)
Predicted Aortic Calcification
0
2
4
6
8
0-1
1-3
3-5
5-7
>7
Manually Anotated Calcification
E)
Probability Density
0.0
0.1
0.2
0.3
0.4
0.5
0.6
0
2
4
6
8
10
12
Predicted Aortic Calcification
B)
Manual annotation = 0
Predicted AAC = 0.18
C)
Manual annotation = 5
Predicted AAC = 4.45
D)
Manual annotation = 12
Predicted AAC = 8.92
F)
Predicted Aortic Calcification
0
2
4
6
8
40
45
50
55
60
65
70
Age

Figure 3

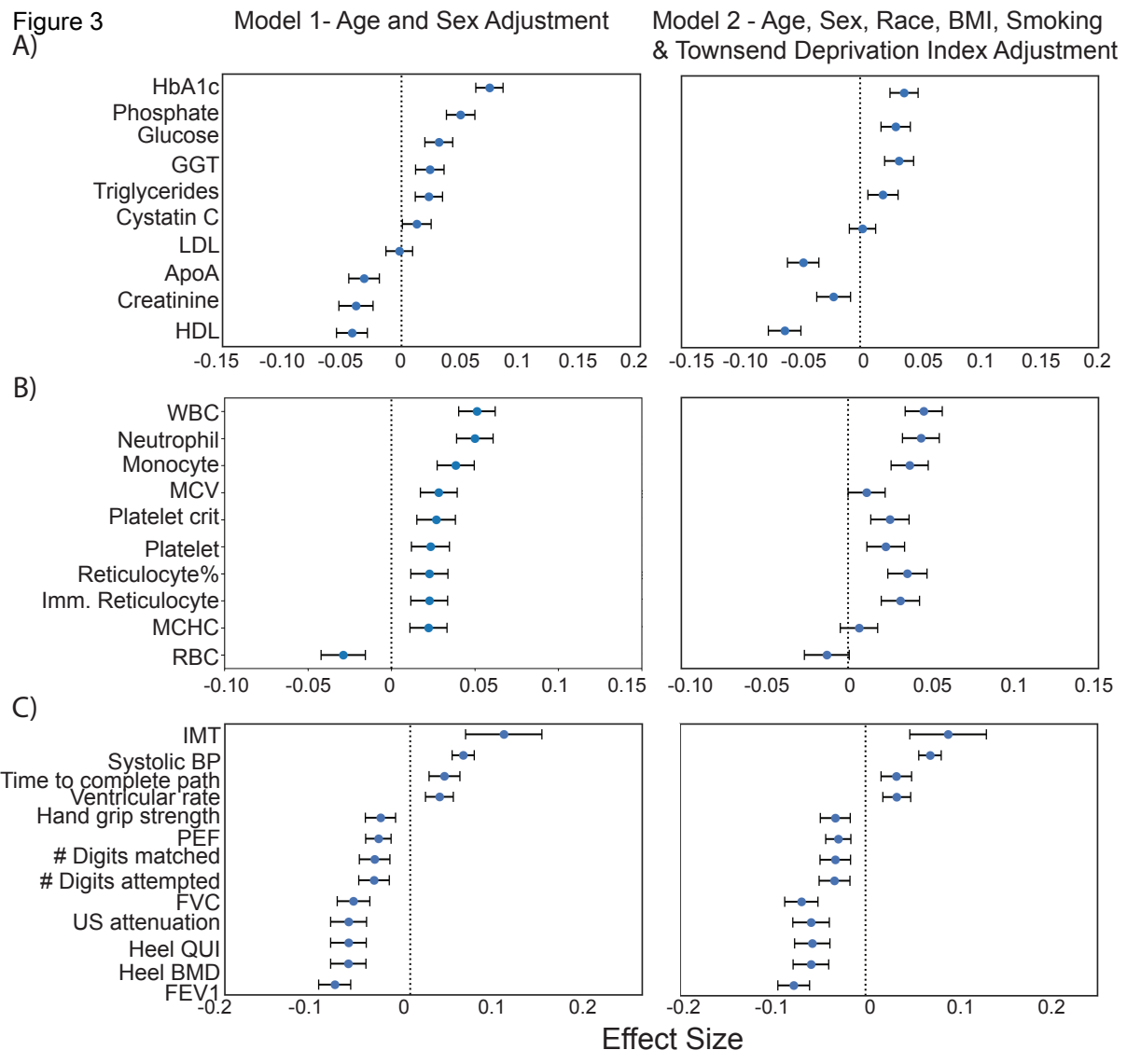
Model 1- Age and Sex Adjustment
Model 2 - Age, Sex, Race, BMI, Smoking & Townsend Deprivation Index Adjustment
A)
HbA1c
Phosphate
Glucose
GGT
Triglycerides
Cystatin C
LDL
ApoA
Creatinine
HDL
-0.15 -0.10 -0.05 0 0.05 0.1 0.15 0.2
B)
WBC
Neutrophil
Monocyte
MCV
Platelet crit
Platelet
Reticulocyte%
Imm. Reticulocyte
MCHC
RBC
-0.10 -0.05 0 0.05 0.1 0.15
C)
IMT
Systolic BP
Time to complete path
Ventricular rate
Hand grip strength
PEF
Digits matched
Digits attempted
FVC
US attenuation
Heel QUI
Heel BMD
FEV1
-0.2 -0.1 0 0.1 0.2
Effect Size

Figure 4

A.

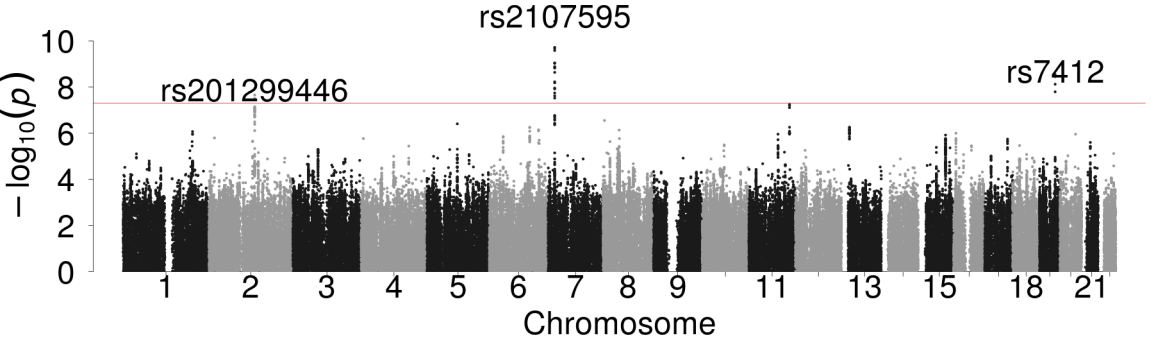
rs2107595
rs201299446
rs7412
$-\log_{10}(p)$
10
8
6
4
2
0
1
2
3
4
5
6
7
8
9
11
13
15
18
21
Chromosome

B.

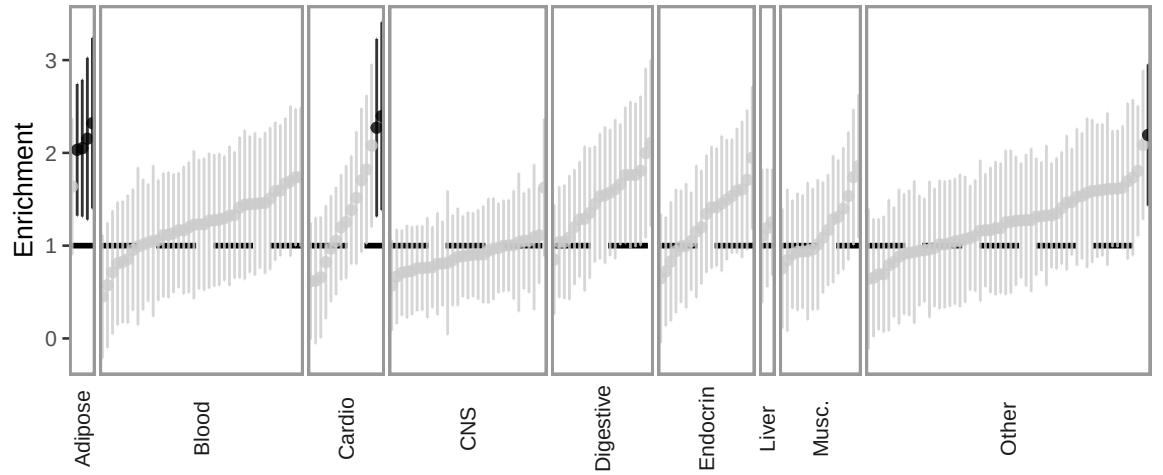
Enrichment
3
2
1
0
Adipose
Blood
Cardio
CNS
Digestive
Endocrin
Liver
Musc.
Other

C.

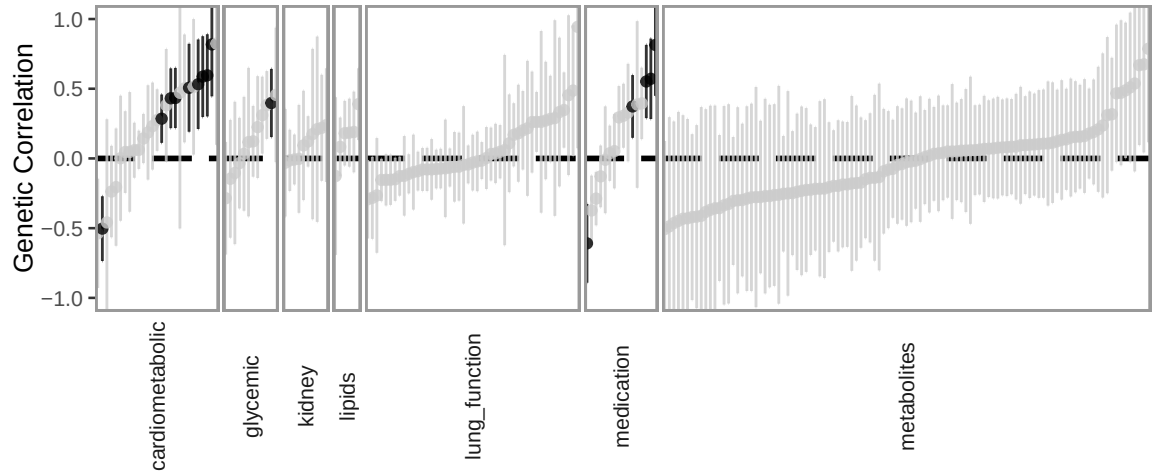
Genetic Correlation
1.0
0.5
0.0
−0.5
−1.0
cardiometabolic
glycemic
kidney
lipids
lung_function
medication
metabolites

Figure 5

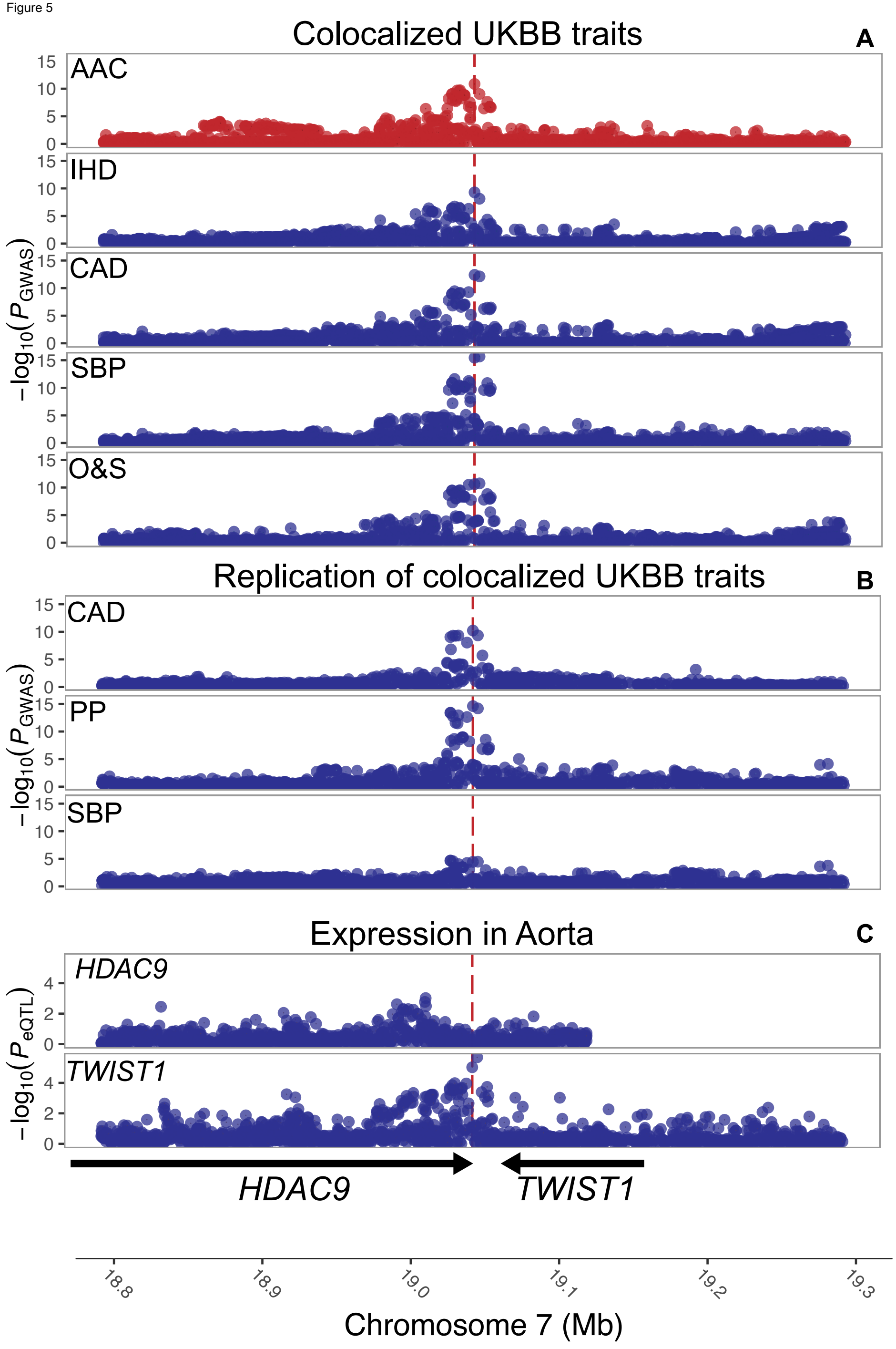
Colocalized UKBB traits
A
AAC
IHD
CAD
SBP
O&S
$-\log_{10}(P_{GWAS})$
Replication of colocalized UKBB traits
B
CAD
PP
SBP
$-\log_{10}(P_{GWAS})$
Expression in Aorta
C
HDAC9
TWIST1
$-\log_{10}(P_{eQTL})$
HDAC9
TWIST1
18.8
18.9
19.0
19.1
19.2
19.3
Chromosome 7 (Mb)

Figure 6

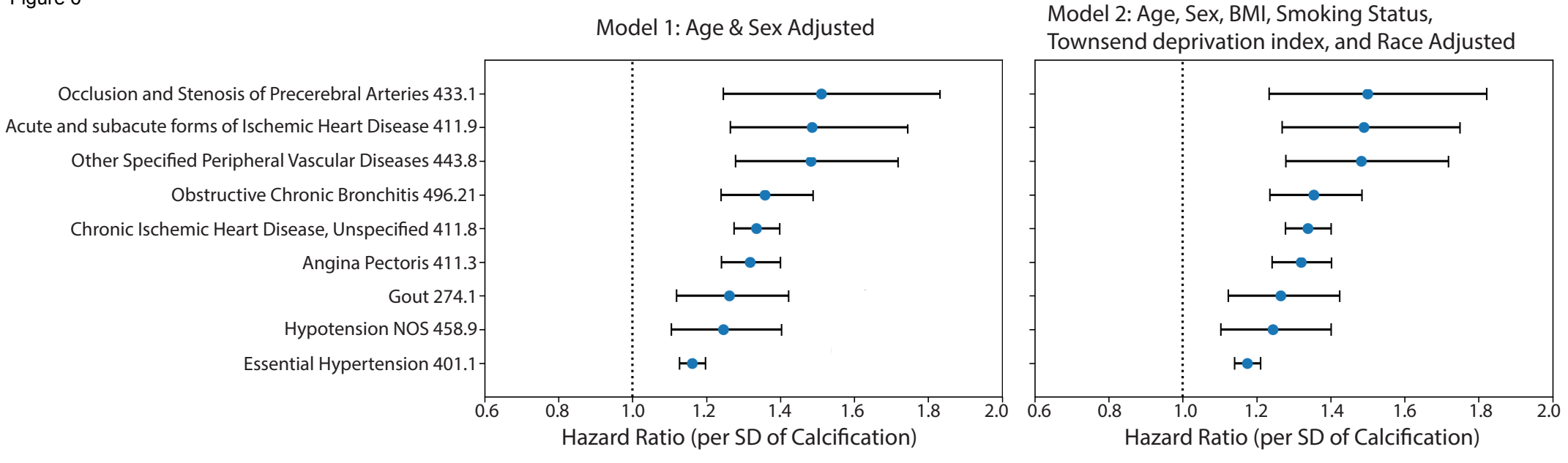
Model 1: Age & Sex Adjusted
Model 2: Age, Sex, BMI, Smoking Status, Townsend deprivation index, and Race Adjusted
Occlusion and Stenosis of Precerebral Arteries 433.1
Acute and subacute forms of Ischemic Heart Disease 411.9
Other Specified Peripheral Vascular Diseases 443.8
Obstructive Chronic Bronchitis 496.21
Chronic Ischemic Heart Disease, Unspecified 411.8
Angina Pectoris 411.3
Gout 274.1
Hypotension NOS 458.9
Essential Hypertension 401.1
0.6
0.8
1.0
1.2
1.4
1.6
1.8
2.0
Hazard Ratio (per SD of Calcification)
Hazard Ratio (per SD of Calcification)

Figure 7

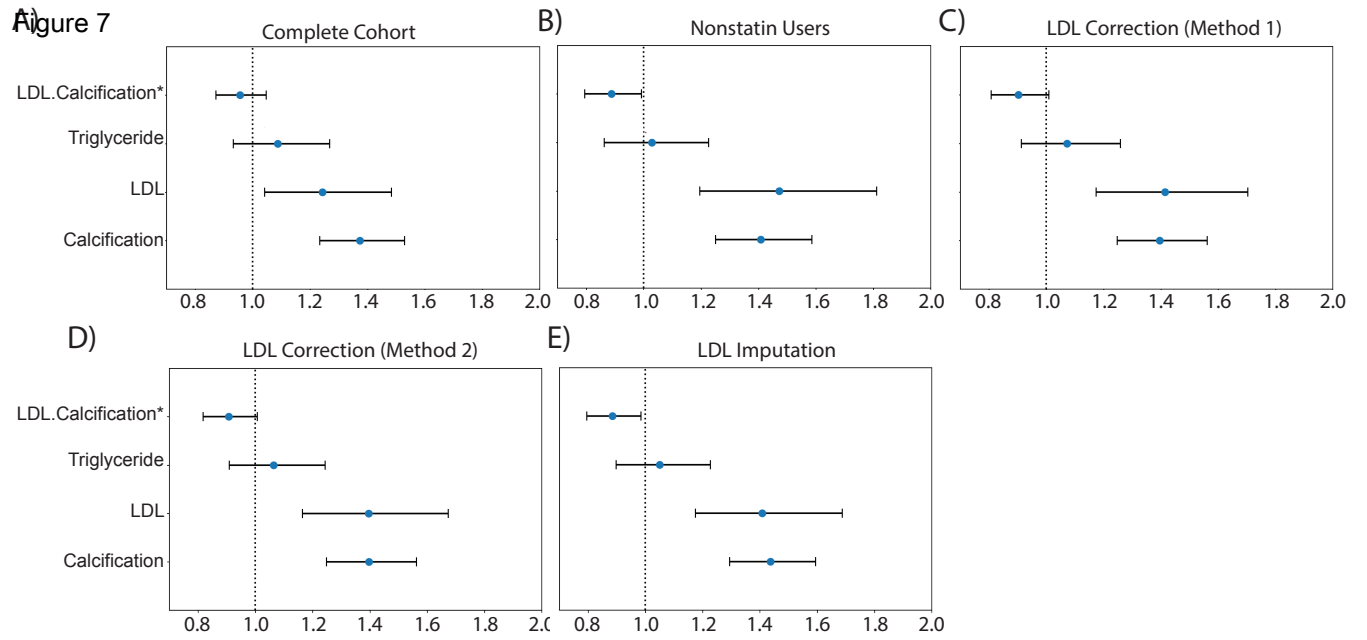
A)
Complete Cohort
B)
Nonstatin Users
C)
LDL Correction (Method 1)
D)
LDL Correction (Method 2)
E)
LDL Imputation
LDL.Calcification*
Triglyceride
LDL
Calcification
0.8
1.0
1.2
1.4
1.6
1.8
2.0